

Pyroelectric Properties and Local Piezoelectric Response of Lithium Niobate Thin Films

Kristina D. Baklanova, Alexander V. Solnyshkin, Inna L. Kislova, Sergey I. Gudkov, Alexey N. Belov,* Vasily I. Shevyakov, Roman N. Zhukov, Dmitry A. Kiselev, and Mikhail D. Malinkovich

In this paper, comprehensive investigation of the pyroelectric properties and local piezoelectric response in ferroelectric film heterostructures is presented. The pyroelectric effect is determined by the dynamic method and the pyroelectric response is recorded for further analysis. It is shown that such studies are effective to analyze the self-polarization phenomena, the stability of the polarized state, the determination of the ferroelectric phase fraction in the film structures, the characterization of grains with in-plane and out-of-plane polarization and others. For example, thin film samples of ferroelectric LiNbO₃ deposited by magnetron sputtering on silicon substrates are considered. The measurement results show that a part of the crystal grains (about 30%) in these films possessed the out-of-plane polarization directed from the free surface to the substrate and determined the peculiarities of the pyroelectric response and the vertical component of the local piezoelectric response.

1. Introduction

Ferroelectric materials integrated in thin film structures have become the basis for a significant improvement in the parameters of existing types of instruments, as well as the creation of a number of new microelectronic devices.^[1–3] The combination of functional properties of bulk materials and nanoscale samples allows creating structures with specified characteristics. Thin ferroelectric layers embedded into heterostructures are of interest both fundamental research and electronic applications. The properties of the film structures

strongly depend on the producing method, electrode materials, and substrate.

Single crystals and ceramics based on niobium oxide compounds are among the dielectric materials used in acousto- and optoelectronics, optics and laser technology, communication, and automation systems. The most important material for these applications is ferroelectric single crystals of lithium niobate (LiNbO₃).^[4] Along with unique optical properties, this material also has thermally stable piezoelectric modules and pyroelectric coefficient. Producing the high quality LiNbO₃ thin films on silicon substrates is particularly attractive.^[5–7] The necessity to study the properties of LiNbO₃ films and their structure is due to a wide range of applications. Promising applications for ferroelectric films are ferroelectric random-access memory (FeRAM),^[8] piezoelectric microelectromechanical systems,^[9] and detection of infrared radiation using the pyroelectric effect.^[10] Moreover, the pyroelectric effect allows to carry out a non-destructive read-out of information recorded in FeRAM.

The aim of this work is to investigate the pyroelectric and local piezoelectric properties of nanostructured thin lithium niobate films deposited on a silicon substrate suitable for the silicon integrated circuit technologies.


2. Experimental Section

The samples of the thin film of LiNbO₃ were deposited by means of magnetron sputtering in a SUNPLA 40TM vacuum chamber (Korea). A Z-cut lithium niobate plate attached to a copper base was used as a target. The deposition was carried out in an argon at a pressure of 0.5 Pa and a magnetron power of 60 W on a silicon substrate of (111) orientation. The substrate was previously cleaned with an ion gun for 5 min. Subsequent annealing was carried out at a temperature of 700 °C for 120 min. The film thickness measured by α -SETM ellipsometer (J.A. Woollam Co., Inc., USA) was 200 ± 1 nm. For studying the pyroelectric properties, copper circular electrodes with diameters 3 mm were deposited on free surface of the film through a metal shadow mask by the magnetron sputtering.

K. D. Baklanova, Prof. A. V. Solnyshkin, Dr. I. L. Kislova, S. I. Gudkov
Tver State University
Tver 170100, Russia

Prof. A. V. Solnyshkin, Prof. A. N. Belov, Prof. V. I. Shevyakov
National Research University of Electronic Technology (MIET)
Moscow, Zelenograd 124498, Russia
E-mail: nanointech@mail.ru

R. N. Zhukov, Dr. D. A. Kiselev, Dr. M. D. Malinkovich
National University of Science and Technology "MISIS"
Moscow 119049, Russia

 The ORCID identification number(s) for the author(s) of this article can be found under <https://doi.org/10.1002/pssa.201700690>.

DOI: 10.1002/pssa.201700690

The phase composition of the films was determined by X-ray diffraction on a DI System diffractometer (Bede Scientific Ltd., UK) in parallel-beam geometry. The X-ray source was an X-ray tube with a copper anode (CuK_α radiation, 40 kV, 40 mA). To increase the intensity of the incident X-ray beam and ensure its partial monochromatization and collimation in the diffraction plane, we used a Göbel mirror. X-ray diffraction patterns were collected in grazing incidence geometry (beam–sample angle on the order of 0.3°), with the sample kept immobile and the detector scanned (2θ axis). Experimental data were analyzed using the EVA program (incorporated into the D8 Discover diffractometer software package) and ICDD PDF-2data.

The dynamic method involves a registration of pyroelectric response caused by periodically modulated heat flux. Semiconductor laser module CLM – 1845 IR – 980 ($\lambda = 980$ nm) was used as a radiation source. Laser power was equal to $P = 220$ mW. IR irradiation was modulated with rectangular shape pulses used in the pyroelectric measurements. The modulation frequency varied from 1 to 10^3 Hz. The modulated heat flux was partially absorbed by the top electrode leading to its temperature change. As a result, polarization of the sample was periodically changed and charges involved in the polarization screening were released. Lock-in amplifier was used to register signal occurring on electrodes.

Topography, as-grown domain structure and local polarization switching study was performed using AC Air Topography mode and Piezoresponse Force Microscopy (PFM) with a commercial atomic force microscopy system MFP-3D Stand Alone (Asylum Research, USA), equipped with high voltage module. Ti/Ir coated conductive soft and hard cantilevers (Asyelec-01 and Asyelec-02, Asylum Research) were used for scanning. Samples poling were performed in the LithoPFM mode by applying a DC voltage to the tip during the scanning. PFM hysteresis loops (“off-loops” or remnant loops) were measured using the SS-PFM mode.^[11]

3. Results and Discussion

X-ray diffraction (XRD) characterization showed that, in the case of cold (111) Si substrates, rf magnetron sputtering produced amorphous LiNbO_3 films (**Figure 1**). After thermal annealing of an as-grown film at 700°C , peaks of LiNbO_3 were detected. The phases present were LiNbO_3 and LiNb_3O_8 . At an annealing temperature of 700°C , a well-defined texture was formed.

It is seen in Figure 1 that annealing at 700°C increased the fraction of LiNbO_3 crystallites whose (001) crystallographic planes were perpendicular to the film surface. In addition to the texturing of the two phases in the film, an increase in the percentage of the former phase and a decrease in that of the latter phase because of diffusion processes might be assumed, but this is less likely because the formation of the LiNb_3O_8 phase attests to lithium deficiency.

It is known that some ferroelectric films exhibit a photovoltaic response to modulated light radiation.^[12–15] In many cases, the observed photovoltaic and photoelectric responses are due to interface effects as well as to optical exchanging the charge of local levels (traps). The results of these studies have shown that the effect of modulated radiation on the $\text{Cu/LiNbO}_3/\text{Si}$

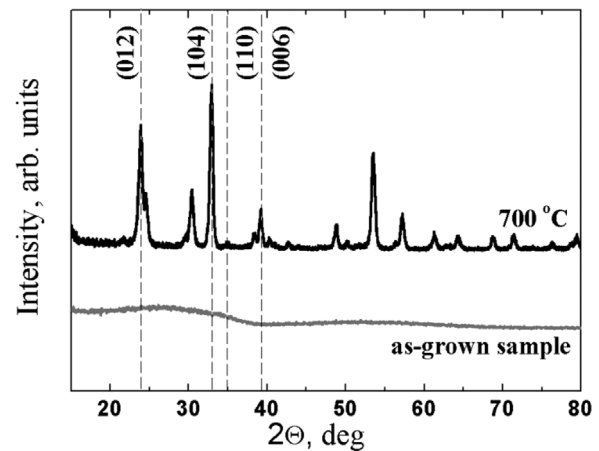


Figure 1. X-ray diffraction patterns of an as-grown LiNbO_3 thin film and film annealing at 700°C .

heterostructure formed by magnetron sputtering leads to the appearance of a signal due to the pyroelectric effect.

The kinetics of the pyroelectric current produced by the action of modulated heat flux on the film sample is presented in **Figure 2**. The upper curve corresponds to time dependencies of the pyroelectric response. The lower curve on the oscillograms is the generator electric signal (U_{dr}) which drives the laser power to create the TTL modulation of the laser beam. The shape of this pulse signal corresponds to the modulation shape of the heat flux. The direction of the pyroelectric current indicates that the polarization of the ferroelectric layer is directed from the top electrode to the substrate.

At low modulation frequencies, the distinctive feature of the response is a significant current spike both at the beginning of the thermal pulse and at its end with its following relaxation to zero (**Figure 2(a)**). For this frequency region, the characteristic thermal time constant (τ_{th}) of the heterostructure is much smaller than the modulation period (τ). As the sample is heated by the irradiation pulse (the light interval), the film temperature increases nonlinearly (near exponentially) and then possesses a stationary value, where the temperature change (ΔT) is equal to zero. While the film temperature changes, the pyroelectric response is observed. The pyroelectric current maximum (the spike amplitude) corresponds to the region of the fastest temperature change. The subsequent relaxation of the pyroelectric current to zero occurs due to a decrease in the heating rate (the temperature change rate), i.e., $dT/dt \rightarrow 0$. After switching off the light (the dark interval), the sample temperature decreases according to the same exponential law and assumes the initial value. As a result, the pyroelectric current reverses the direction, while its temporal behavior corresponds to the current kinetics for the light interval. A detailed discussion and calculation of the temperature change and its rate for a ferroelectric heterostructure under the modulated radiation action are presented in Ref. ^[16].

At frequencies above 20 Hz, the response does not relax to zero and a constant component of the response appears (**Figure 2b and c**). In the frequency range of about 20–200 Hz, the characteristic thermal time constant of the heterostructure

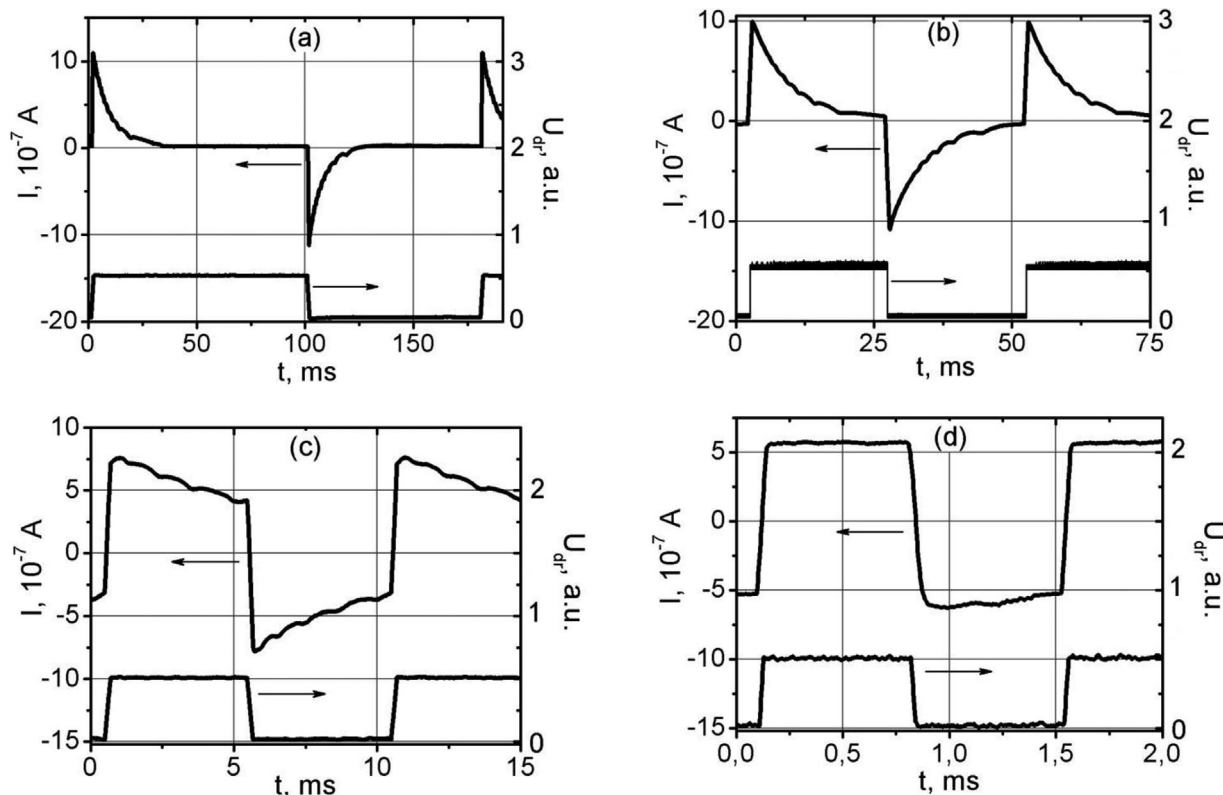


Figure 2. Oscillograph traces of the pyroelectric current (upper curves) of LiNbO₃ film at various modulation frequencies of the IR irradiation: a – 5, b – 20, c – 100, d – 700 Hz.

corresponds in order of magnitude to the modulation period. For the light and dark intervals, the film temperature increases and decreases nonlinearly also, but does not reach the stationary value. Therefore, the pyroelectric current does not relax to zero.

At higher frequencies (more than 500 Hz), the signal shape becomes rectangular (Figure 2(d)). This frequency range is characterized by the periods much less than the characteristic thermal time constant. During both the light and dark intervals, the time dependences of the film temperature are linear. Therefore, the pyroelectric response has a stationary (time independent) component, since the pyroelectric current is constant for small temperature variations at the linear heating or cooling.

Such a behavior of the response induced by the modulated thermal flux allows concluding about its pyroelectric origin. The change of the response amplitude by a factor of two with increasing modulation frequency from 1 to 500 Hz is another confirmation of the pyroelectric nature. This occurs due to the transition from a single pulse mode (low frequencies) to a regular heating mode (high frequencies) when the signal does not change during the action of the thermal pulse.^[17]

The frequency dependence of the amplitude value of the response was plotted on the basis of oscillograms obtained at different frequencies of the heat flux modulation (Figure 3). The frequency (f) of the generated signal varied from 1 to 10³ Hz. As one can see from the obtained dependences, the response value for the dark interval (curve 2) is $\approx 0.9 \times 10^{-7}$ A greater than for

the light interval (curve 1). At low modulation frequencies (1–20 Hz), the frequency dependences of the response amplitude remain practically unchanged for both the light and dark intervals and the amplitude is about 1.2×10^{-6} A. For the thin film structure, this modulated heat flow effect corresponds to the single-pulse mode since $\tau \gg \tau_{th}$.

In the frequency range 20–300 Hz, the current amplitude value monotonically decreases to 0.64×10^{-6} A in accordance with near linear law on a semilogarithmic scale. The transition of

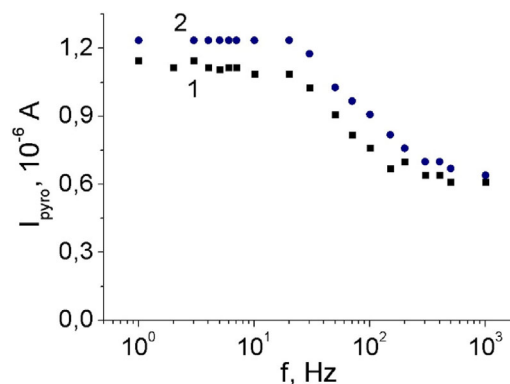


Figure 3. Frequency dependence of the pyroelectric current amplitude. Curve 1 corresponds to the signal amplitude for light on and curve 2 corresponds to the one for light off.

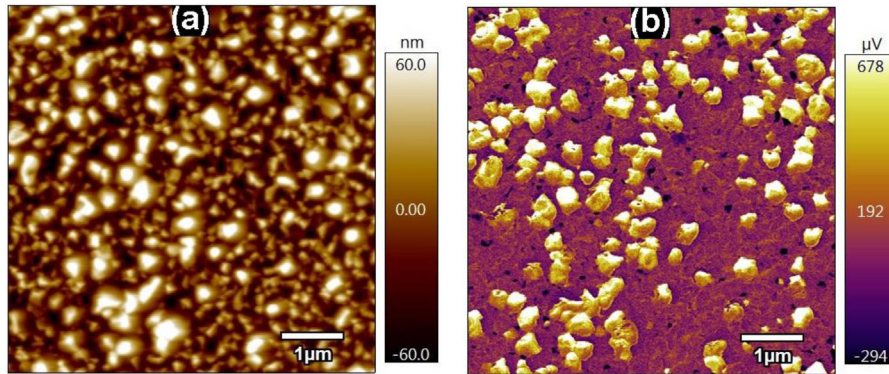


Figure 4. Topography of the thin film surface of lithium niobate obtained by the atomic force microscopy method (a) and surface distribution of the piezoelectric response obtained by the PFM mode (b).

the single pulse mode to the regular heating mode occurs in this frequency domain. At high frequencies of the laser beam modulation ($f > 300$ Hz), the current value remains invariable and is equal to $\approx 0.64 \times 10^{-6}$ A. This frequency interval corresponds to the condition $\tau \ll \tau_{th}$ which determines the regular heating mode. Such a frequency dependence of the current amplitude value is characteristic for the pyroelectric signal which confirms the pyroelectric activity and the presence of the out-of-plane polarization in the LiNbO_3 layer.

On the basis of experimental data, the pyroelectric coefficient of the ferroelectric film of lithium niobate was calculated according to the following relationship^[18]:

$$p = \frac{2I c d}{\eta P} \quad (1)$$

where I is pyroelectric current, $c = 2.92 \times 10^6 \text{ J m}^{-3} \text{ K}^{-1}$ corresponds to LiNbO_3 film heat capacity, d the film thickness, $\eta = 0.1$ the copper electrode absorption constant in near infrared region, $P = 220 \text{ mW}$ the laser radiation power. Calculations were carried out for high frequency part of pyroelectric response (which corresponds to quasi-stationary component of pyroelectric response). The calculated value of the pyroelectric coefficient was $\approx 3.2 \times 10^{-5} \text{ C m}^{-2} \text{ K}^{-1}$ which is ≈ 3 times less than the one given in the literature for a LiNbO_3 single crystal.^[19] Such a discrepancy may be associated with either a small content of the ferroelectric phase in the film sample or different orientations of the polarization vectors in individual LiNbO_3 grains comprising the film.

For a more detailed analysis of the pyroelectric activity, the study of local polarization of the LiNbO_3 films was carried out by the piezoelectric force microscopy (PFM). **Figure 4** shows the film surface image and a vertical signal of the piezoelectric response.

As seen from **Figure 4(a)**, the film has a grain structure with a typical grain size of about 200–300 nm. The color contrast in **Figure 4(b)** is related to the amplitude and direction of the local piezoelectric response. The light regions correspond to the piezoelectric signal associated with the polarization direction from the surface to the substrate in the grains. This out-of-plane polarization determines the pyroelectric response of the film structure. For a comparative characterization of the polarization

over the film surface, the intensity of the vertical component of the piezoelectric response (Vertical PFM) was found (**Figure 5**).

According to the response histogram, the distribution of the vertical signal has two maxima corresponding to ≈ 0 and $\approx 250 \text{ mV}$. The nearly zero signal corresponds to nonferroelectric grains or grains with the polarization direction along the film surface (the in-plane polarization). These grains cannot contribute to the pyroelectric response or exhibit very weak pyroelectricity. On the basis of the distribution of the piezoelectric response, one can conclude that the vertical component of the summary polarization in the LiNbO_3 films is directed from the free surface to the substrate. It is essential to note that the pyroelectric response phase induced by the modulated heat flux indicates the same direction of the out-of-plane polarization determining the local piezoelectric effect.

Finally, remnant loops have been received on the samples using switching spectroscopy PFM (SS-PFM). Hysteresis in PFM is fundamentally different than hysteresis in a macroscopic sample (**Figure 6**). Macroscopic hysteresis occurs due to the nucleation growth and interaction of multiple separated domains, while in PFM, nucleation of a single domain occurs under a sharp tip and PFM signal follows the development of domains at a single location. Here, the remanent piezoelectric

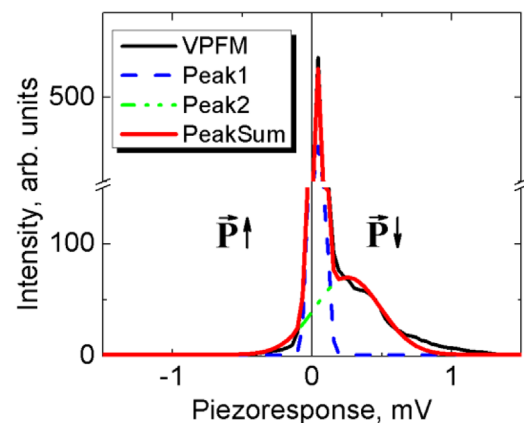


Figure 5. The histogram of the piezoelectric signal distribution over the scanned area of the LiNbO_3 film.

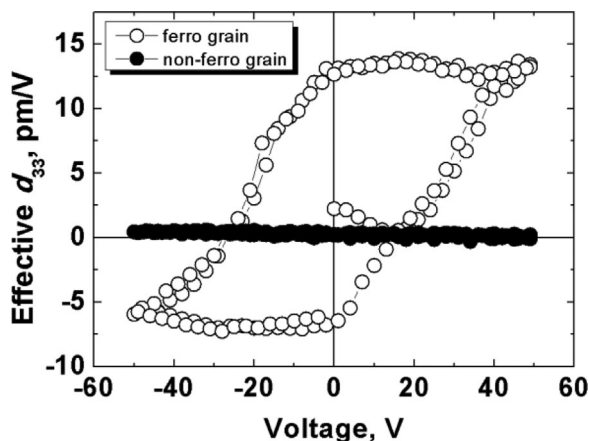


Figure 6. PFM hysteresis loops in ferro-activity (open circles) and non-ferro activity (solid circles) grains for LiNbO₃ thin film.

response has been measured in 30 ms after the removal of the DC pulse (duration 30 ms).

The effective d_{33} were derived from $d_{33} = \text{PFM}_{\text{ampl}} \cdot \cos(\text{Phase})$ as shown in Figure 6. The offset of d_{33} hysteresis loop for ferroelectrically active grain could be attributed to the presence of non-switchable domains pinned near the electrode-film interface and built-in electric field (imprint),^[20] which resulted from the difference nature of the top (Ti/Ir tip) and bottom electrodes. Values of remanent d_{33} were found to be 12.5 pm V^{-1} . For non-ferroelectrically active grains, the d_{33} hysteresis loop was not obtained, the signal was around zero.

4. Conclusions

The topography and the local piezoelectric response distribution over the surface of ferroelectric lithium niobate films deposited on a silicon substrate were obtained. The study showed the presence of a grain structure in these films. There are two types of the grains in LiNbO₃ layers. The first type grains were pyroelectrically active and revealed the significant vertical component of the local piezoelectric response. It was experimentally found that these grains were self-polarized and their polarization was directed from the free surface to the substrate. Grains of the second type did not generate the noticeable vertical PFM and, therefore, could not exhibit any significant pyroelectric effect. These grains might either have no the ferroelectric polarization (nonferroelectric phase) or possess the in-plane polarization. The latter is more probable, since the content of the other crystalline phase like LiNb₃O₈ is small according to the XRD data.

The dynamic method was used to study pyroelectric properties of the LiNbO₃ films. It was shown that the pyroelectric coefficient of the ferroelectric layers could be calculated in accordance with the high-frequency response induced by the periodically modulated heat flux. In the high frequency region ($f > 300 \text{ Hz}$), the pyroelectric response had the rectangular shape that made it possible to determine the pyroelectric coefficient. For these LiNbO₃ films, the calculated value was equal to $3.2 \times 10^{-5} \text{ C m}^{-2} \text{ K}^{-1}$. It means that ferroelectric grains in an

amount of $\approx 30\%$ possess the out-of-plane polarization. From PFM measurements of the remanent d_{33} were found to be 12.5 pm V^{-1} .

Thus, the comparative studies of the dynamic pyroelectric effect and local piezoelectric activity allow to determine the total polarization perpendicular to the ferroelectric film plane and, as a consequence, the grain fractions with different polarization directions. Also, it is necessary to determine the in-plane polarization and to consider its contribution to the pyroelectric response due to thermal deformations of substrates in the sequel. The research presented above allows to check ferroelectric heterostructure quality and to develop recommendations for the further improvement of ferroelectric film production. Further studies of these questions are in progress.

Acknowledgment

This work was supported by the Russian Scientific Foundation (Grant No. 15-19-00138).

Conflict of Interest

The authors declare no conflict of interest.

Keywords

lithium niobate thin films, piezoelectric response, pyroelectric properties

Received: September 7, 2017

Revised: October 21, 2017

Published online:

- [1] A. K. Bain, P. Chand, *Ferroelectrics: Principles and Applications*. Wiley-VCH, Berlin **2017**, p. 328.
- [2] P. Muralt, *J. Micromech. Microeng.* **2000**, *10*, 136.
- [3] N. Settera, D. Damjanovic, *J. Appl. Phys.* **2006**, *100*, 051606.
- [4] T. Volk, M. Wöhlecke, *Lithium Niobate: Defects, Photorefraction and Ferroelectric Switching*. Springer Science & Business Media, Luxembourg **2008**, p. 250.
- [5] J. Lin, J. Chen, K. S. Ho, T. A. Rabson, *Integr. Ferroelectr.* **1995**, *11*, 221.
- [6] Y.-B. Park, B. Min, K. J. Vahala, H. A. Atwater, *Adv. Mater.* **2006**, *18*, 1533.
- [7] P. O. Weigel, M. Savanier, C. T. DeRose, A. T. Pomerene, A. L. Starbuck, A. L. Lentine, V. Stenger, S. Mookherjee, *Sci. Rep.* **2016**, *6*, 22301.
- [8] S. Moon, D. Lim, B. Jang, J. Yi, *Proceedings of the 12th IEEE ISAF* **2000**, 1013, **2000**.
- [9] H. Bhugra, G. Piazza, *Piezoelectric MEMS Resonators*. Springer Nature, Cham, Switzerland **2008**, p. 423.
- [10] R. H. Sarker, H. Karim, R. Martinez, N. Love, Y. Lin, *IEEE Sens. J.* **2016**, *16*, 5883.
- [11] S. Jesse, A. P. Baddorf, S. V. Kalinin, *Appl. Phys. Lett.* **2006**, *88*, 062908.
- [12] A. A. Bogomolov, A. V. Solnyshkin, D. A. Kiselev, I. P. Raevskii, N. P. Protzenko, D. N. Sandzhiev, *Phys. Solid State* **2006**, *48*, 1192.
- [13] A. A. Bogomolov, A. V. Solnyshkin, D. A. Kiselev, I. P. Raevsky, N. P. Protzenko, D. N. Sandjiev, *J. Eur. Ceram. Soc.* **2007**, *27*, 3835.
- [14] A. A. Bogomolov, A. V. Solnyshkin, M. V. Shilov, G. Suchanek, *Bull. Russian Acad. Sci.: Phys.* **2010**, *74*, 1307.

- [15] M. V. Shilov, A. A. Bogomolov, A. V. Solnyshkin, *Bull. Russian Acad. Sci.: Phys.* **2011**, 75, 1403.
- [16] A. V. Solnyshkin, A. A. Bogomolov, D. Yu. Karpenkov, I. L. Kislova, A. N. Belov, *Tech. Phys.* **2016**, 61, 541.
- [17] A. A. Bogomolov, A. V. Solnyshkin, A. V. Kalgin, A. G. Gorshkov, S. A. Gridnev, *Bull. Russian Acad. Sci.: Phys.* **2011**, 75, 1367.
- [18] A. V. Solnyshkin, I. M. Morsakov, A. A. Bogomolov, A. N. Belov, M. I. Vorobiev, V. I. Shevyakov, M. V. Silibin, V. V. Shvartsman, *Appl. Phys. A.* **2015**, 121, 311.
- [19] S. T. Popescu, A. Petris, *J. Appl. Phys.* **2013**, 113, 043101.
- [20] S. V. Kalinin, B. J. Rodriguez, S. Jesse, E. Karapetian, B. Mirman, E. A. Eliseev, A. N. Morozovska, *Annu. Rev. Mater. Res.* **2007**, 37, 189.